a) Preparation Procedures for Vinyl Acetate-1-^{13}C[1] and Corresponding Spectra

Procedure_1:

To a round bottom distillation flask (250 mL) equipped with a magnetic stir bar ruthenium (III) chloride hydrate (0.05 eq., 4.9 mmol, 1.01g), sodium acetate-1-^{13}C (0.065 eq., 6.4 mmol, 0.53 g, 98% isotopic purity), vinyl laurate (4 eq., 392 mmol, 102 mL), acetic acid-1-^{13}C (98.0 mmol, 6.00 g, 98% isotopic purity) were added. The flask was attached to distillation apparatus: distillation column (Vigreux), 3-way distillation connecting adapter with mercury thermometer on top, distillation condenser (water), distillation adapter with vacuum takeoff and a round bottom collection flask (25 mL). The system was put under inert atmosphere of argon by temporary replacing the thermometer with rubber septum penetrated by a needle, which in turn was connected to the argon gas line. Please note that "vacuum takeoff" is used as gas exhaust during this procedure. After 30 minutes, the thermometer was quickly returned to its place and the "vacuum takeoff" was plugged with rubber septum. Two needles (one connected to the argon line and the other one opened to atmospheric pressure) were inserted into the septum. This setup keeps the system under inert gas, while avoiding pressure buildup. The collection flask was cooled on ice bath. The distillation flask was heated to 140 °C by a heating mantel connected to a heating apparatus equipped with thermocouple. After 30 min, distillation of the product started to accumulate in the collection flask. Two hours later, distillation was completed furnishing vinyl acetate-1-^{13}C (8.87 g, 102 mmol, 98%* based on combined load of sodium acetate-1-^{13}C and acetic acid-1-^{13}C). * The actual yield of the product was lower due to the presence of ethyl acetate-1-^{13}C (~3 mol %) and acetaldehyde with natural isotopic abundance (~20 mol %). (*Note that acetaldehyde can be removed by means of fractional distillation*)

Procedure_2 (low catalyst load):

The alternative procedure has the same basic steps and setup (above) and differs only in reagents loads as well as in the yield and purity of the product. Thus, ruthenium (III) chloride hydrate (0.02 eq., 2.0 mmol, 0.406 g), sodium acetate-1-^{13}C (0.032 eq., 3.2 mmol, 0.53 g, 98% isotopic purity), vinyl laurate (3 eq., 294 mmol, 77 mL), acetic acid-1-^{13}C (98.0 mmol, 6.00 g, 98% isotopic purity) were used. Yield of vinyl acetate-1-^{13}C was 31% (2.8 g, 32 mmol).

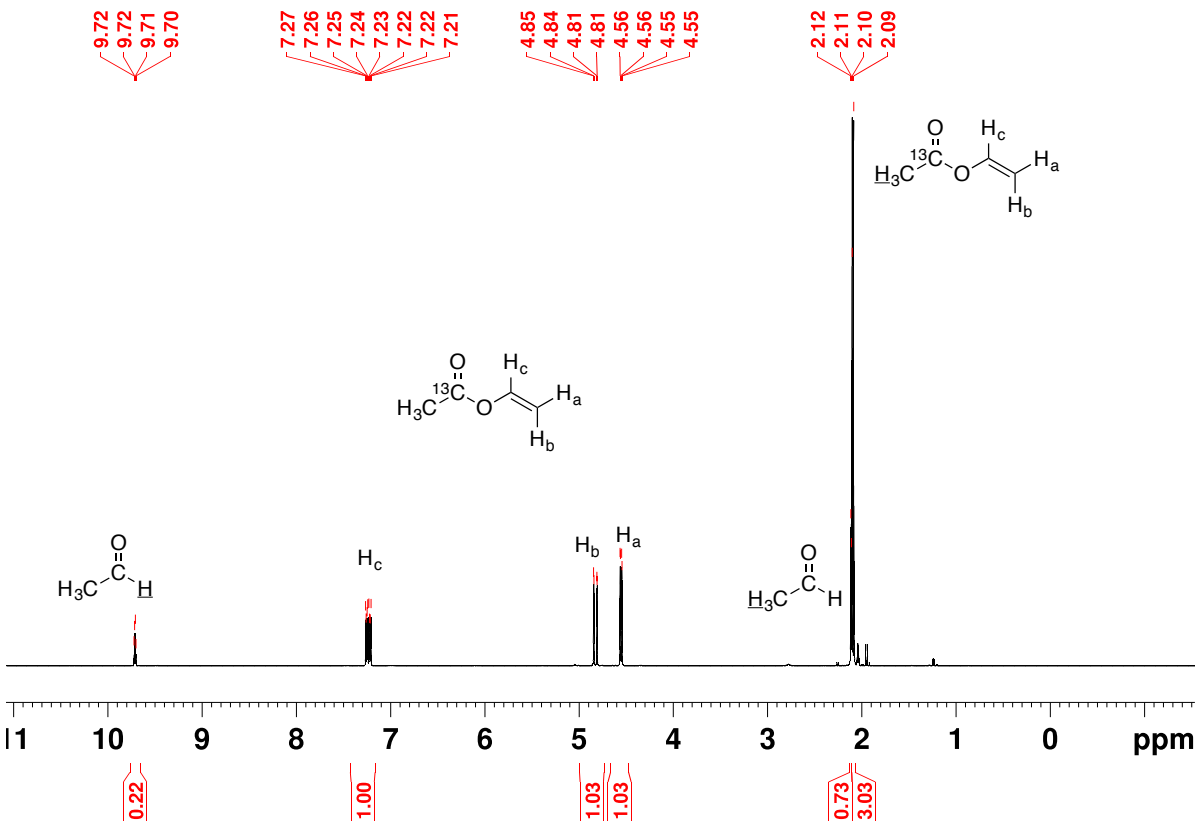

Figure S1. High-resolution proton NMR spectrum of **vinyl acetate-1-^{13}C** (Procedure_1) containing ~3 mol % of **ethyl acetate-1-^{13}C** and ~20 mol % **acetaldehyde** (with natural isotopic abundance) in acetone-d_6 recorded using Bruker 400 MHz NMR spectrometer.

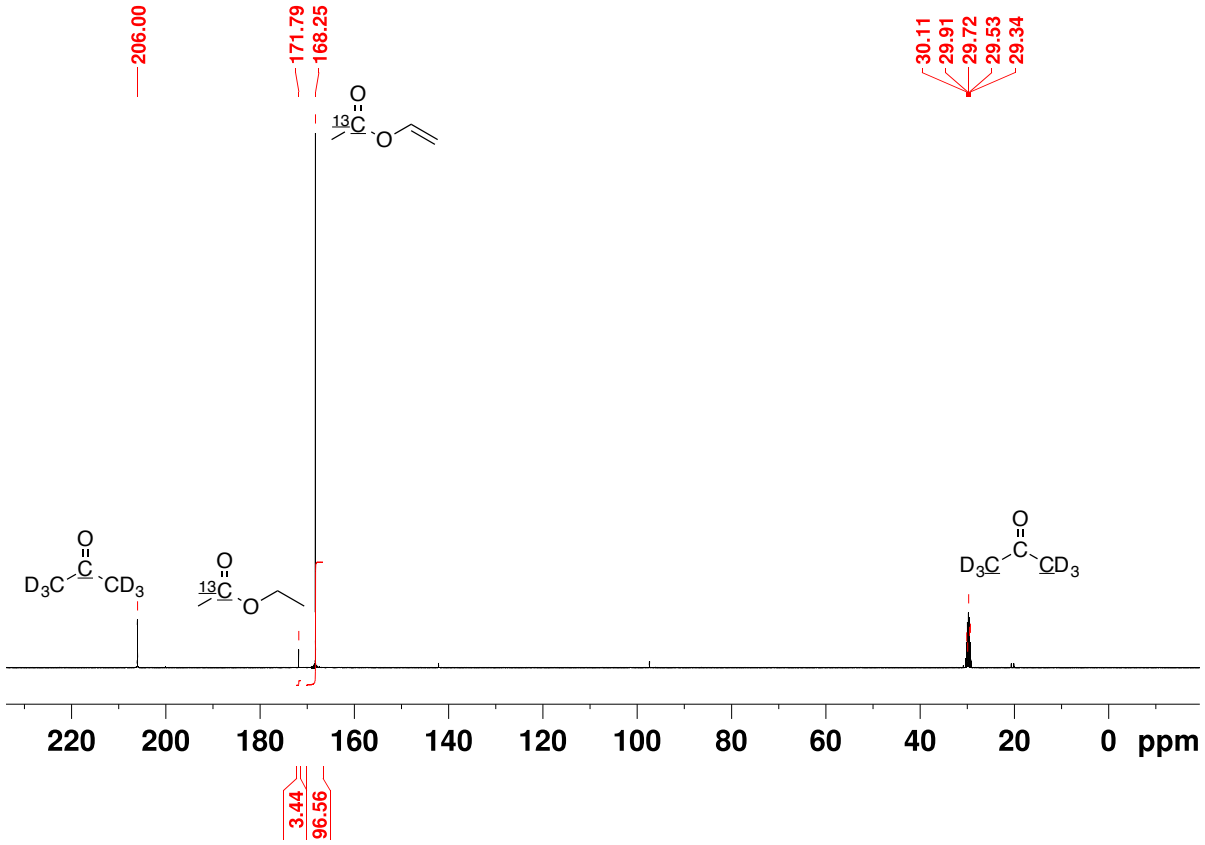

Figure S2. High-resolution $^{13}C\{^{1}H\}$ NMR spectrum of **vinyl acetate-1-^{13}C** (Procedure_1) containing ~3 mol % of **ethyl acetate-1-^{13}C** and ~20 mol % **acetaldehyde** (with natural isotopic abundance) in acetone-d_6 recorded using Bruker 400 MHz NMR spectrometer.

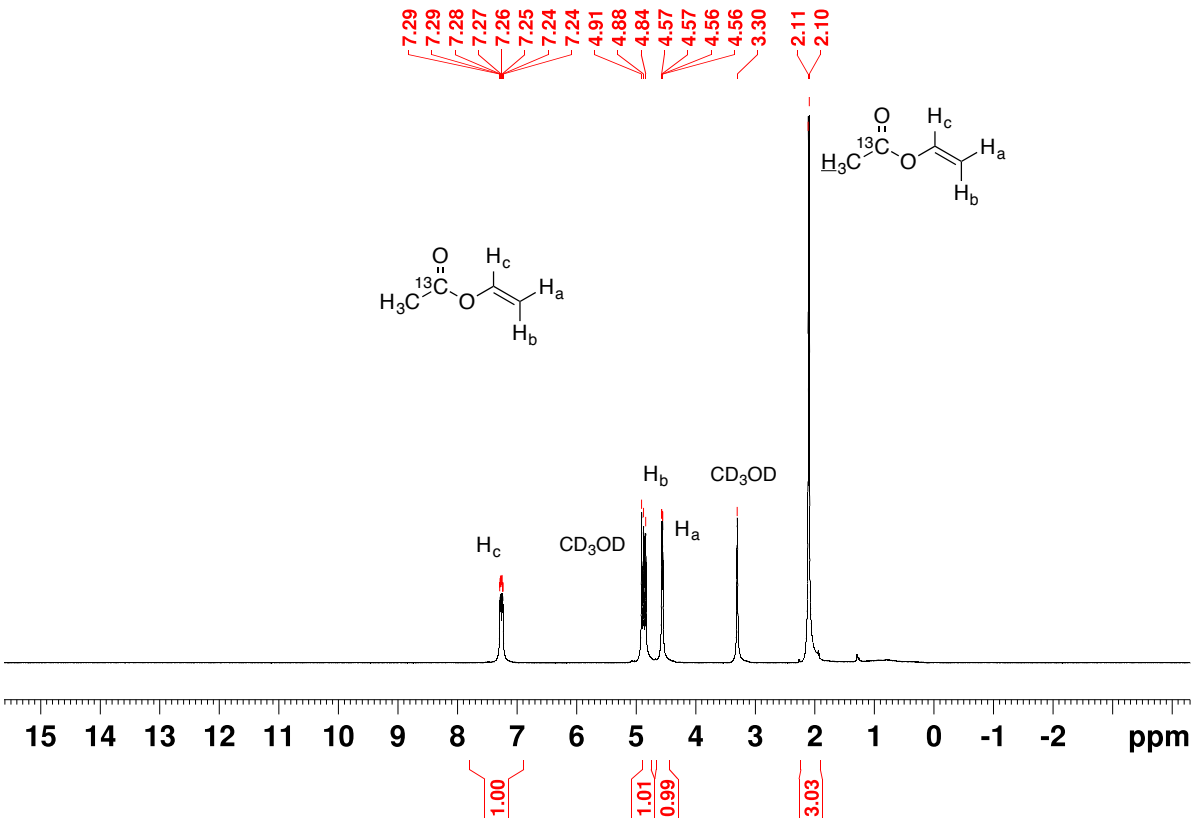

Figure S3. High-resolution proton NMR spectrum of pure **vinyl acetate-1-^{13}C** (Procedure_2) in methanol-d_4 recorded using Bruker 400 MHz NMR spectrometer.

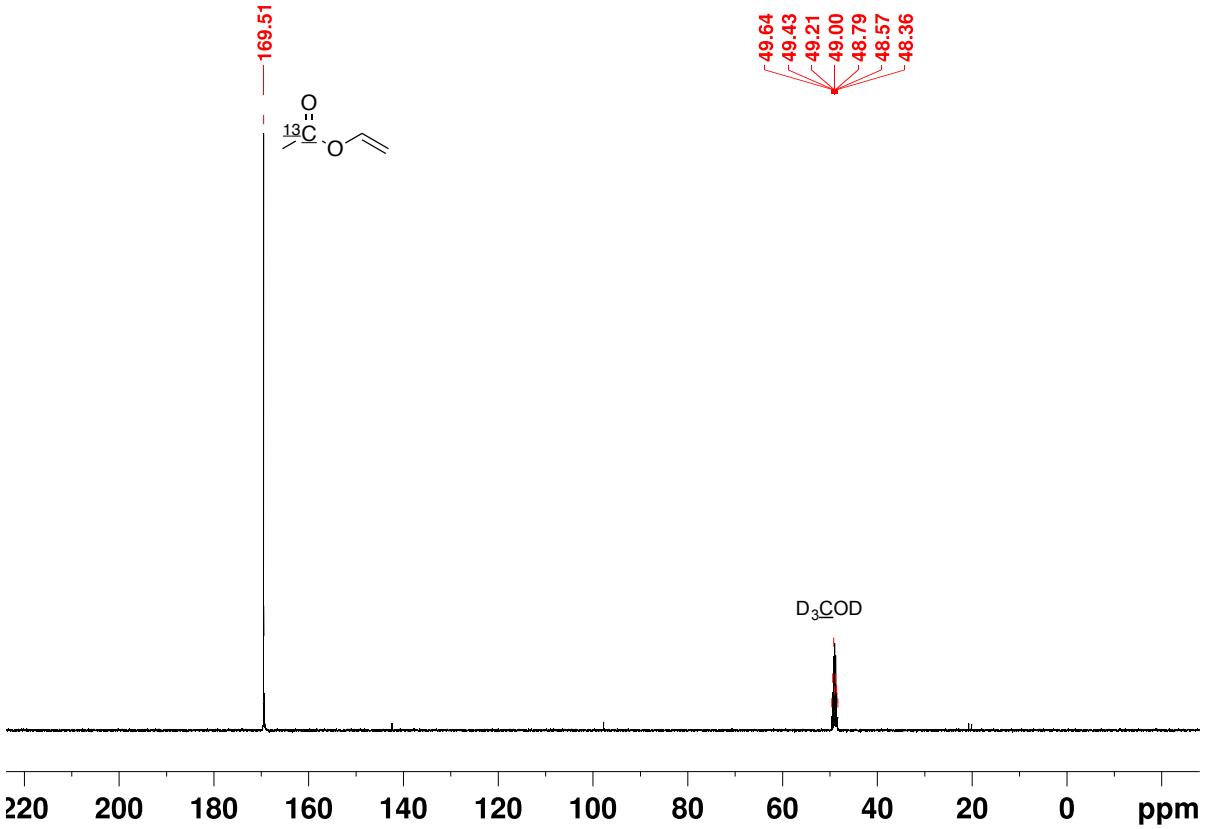

Figure S4. High-resolution $^{13}C\{^{1}H\}$ NMR spectrum of pure **vinyl acetate-1-^{13}C** (Procedure_2) in methanol-d_4 recorded using Bruker 400 MHz NMR spectrometer.

b) Preparation of Catalyst Containing Solution for Pairwise *Para*-H_2 Addition to Vinyl Acetate or Vinyl Acetate-1-^{13}C

Methanol-d_4 (20 mL) was placed in 25 mL vial with Teflon cap and degassed by repetitive (5 times) sequence: argon flushing, closing cap, vortexing. Rhodium catalyst [(Bicyclo[2.2.1]hepta-2,5-diene)[1,4-bis(diphenylphosphino)butane]rhodium(I) tetrafluoroborate, 0.1 mmol, 0.708 g] and vinyl acetate (1.6 mmol, 0.139 g for vinyl acetate-1-^{13}C) were added and the vial was vortexed until all the solid particles dissolved. The resulting solution was placed in prefilled with argon medium-wall NMR tubes (0.5 mL each).

c) Experimental Setup for Hyperpolarization, PHIP-SAH experiments and Magnetic Field Cycling

The experimental setup for PHIP-SAH, exclusive of the high-field NMR spectrometer, is not instrumentation demanding. As seen in Figure S5, *para*-H_2 with 50% *para*-state purity is produced by flow of bulk H_2 through a spiral of 1/4 in. copper tubing (P/N 5174K21, McMaster-Carr) filled with sufficient quantity of FeO(OH) catalyst (P/N 371254, Sigma-Aldrich) to achieve a 60 cm packed length of catalyst. The spiral was placed within a liquid N_2 bath with the H_2 regulator pressure set to 120 psi, near the mass flow controller's (MFC) pressure limit (SmartTrak 50, Sierra Instruments, Monterey, CA). The MFC connects to a gas manifold consisting of a medium-wall high-pressure NMR tube into which a 1/16 in. OD PTFE capillary tube is inserted, a manual valve, a

pressure gauge, and a check safety valve set to 90 psi. With the manual valve open, *para*-H_2 passing through the MFC exits the check safety to the vent and the pressure difference across the NMR tube solution is zero, corresponding to no bubbling. With the valve closed, *para*-H_2 bubbles through the NMR tube solution to the vent. An experiment thus consists of commencing bubbling, magnetic field cycling the solution as depicted in Main Text Figure 1d, and terminating bubbling followed by adiabatic passage from the shield to the 9.4T spectrometer for detection.

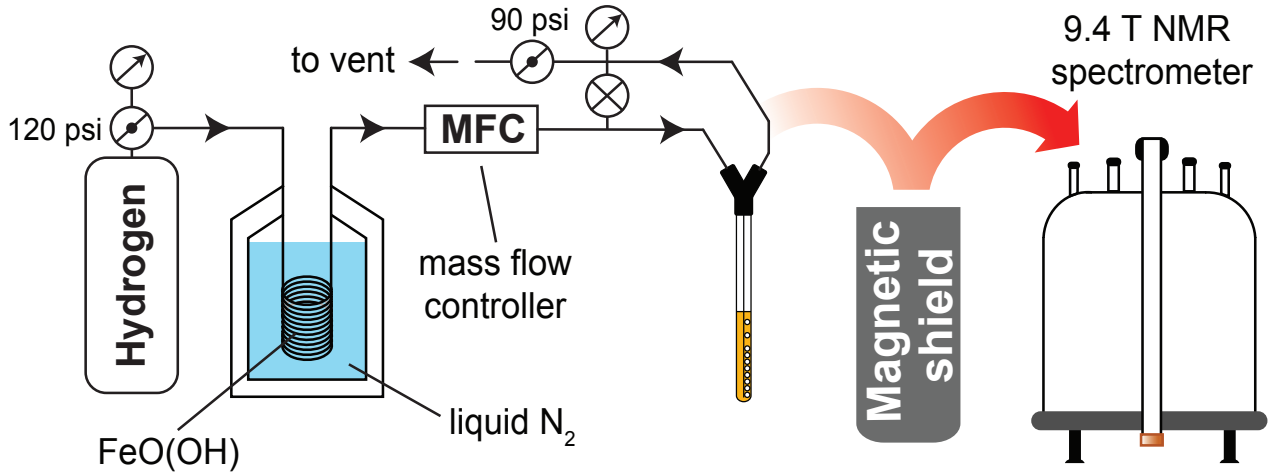

Figure S5. Schematic representation of experimental setup for hydrogenation with magnetic field cycling. Hydrogenation with *para*-H_2 is carried out at the Earth's magnetic field, produced in line by using *para*-H_2 generator operating at the temperature of liquid nitrogen (77 K). Mass flow controller (MFC) was set to the value of 80 sccm and provided continuous *para*-H_2 flow during the whole set of experiments. When the downstream valve is open the gas passes by the sample and leaves through the vent. When the valve is closed, the gas flow goes through the reaction solution. Advantage of this approach in comparison with standard "valve-closing" approach is that it prevents residual bubble formation and thus, one doesn't need to wait for additional delay before spectrum acquisition. Once hydrogenation is completed, the valve is closed and the sample is then quickly moved inside μ-metal shield (with reduced magnetic field for cycling B_{FC}) and slowly transferred from the shield for subsequent NMR detection. The latter procedure provides efficient polarization transfer from *para*-H_2-nascent protons to heteronuclei present in the molecule.

For the field cycling experiment, a magnetic shield setup as devised originally by Theis et al. was used consisting of three concentric cylinders of MuMETAL (P/N ZG-206, Magnetic Shield Corporation, Bensenville, IL). Inside the shield an optimal magnetic field strength was generated with a solenoid coil: a 7 in. long basket-weave solenoid coil[2] wound so that it was centered on a 12 in. long and ~4 in. diameter G12 fiberglass tube (P/N G12-4I-VL, Rocketry Warehouse, Hollsopple, PA). Whereas magnet wire would be more suitable for DC currents, this coil on hand used Litz wire construction (SKU 125/40-Litz, Mike's Electronic Parts, Fairfield, OH). Albeit buying the shield with the degaussing coil option is recommended in hindsight, a degaussing coil was constructed of 20 AWG magnet wire composing two end rings and a broad central segment wound in between the cylinder spacers welded to the innermost cylinder.

It is important to note that the MuMETAL shield is magnetized when delivered, necessitating degaussing before use. The degaussing procedure entails increasing the degaussing field strength to a sufficiently high level and then smoothly ramping the field back down. Field ramping was enabled through use of a Superior Electric 3PN116C POWERSTAT Variable Transformer (P/N 32M1447, Newark element14, Palatine, IL). This variac was found to achieve continuous variation of the applied voltage (i.e. no discrete steps deleterious to the degaussing procedure). A Lakeshore 410 Gaussmeter (P/N 410-HCAT, Lake Shore Cryotronics Inc, Westerville OH) was used to measure the solenoid coil's magnetic field strength during calibration. For the degaussing procedure, first the magnetic field as measured axially was ramped up to 80 G (near the variac's 10 A current limit). Then the applied field was very slowly decreased back to zero. It is estimated that the residual

magnetization in the shield in conjunction with the attenuated Earth field of 50 μT is < 0.1 μT following the degaussing procedure.

Besides the magnetic shield and solenoid coil described above, the experimental setup entailed creating an electrical circuit involving other components including a power supply unit (PSU) and a variable resistance all connected electrically in series with the solenoid coil. For the PSU a GW Instek GPR-3060D (ASIN B005G038PI, Amazon.com) was used. For the variable resistance a resistor decade box (P/N 510-RDB-10, Mouser Electronics, Mansfield, TX) permitted easily changing the total circuit resistance in discrete steps.

In order to enable efficient polarization, the magnetic field strength generated by the solenoid needs to be set optimally, and thereby necessitating calibration of the magnetic field strength. To achieve this, first the resistor decade box in series with the solenoid was set to 10 Ω and the PSU was set to 10 V. From this baseline, an axial magnetic field of ~5.7 G was measured within the solenoid inside the shield. By application of Ohm's law, this measurement therefore indicates that a magnetic field strength of 0.57 μT is generated for 1V set on the PSU and with the decade box set to 1 kΩ. Therefore, the magnetic field calibration was ~0.57 μT/kΩ/V, with any changes in the desired field strength enabled by simply altering the setting on the resistor decade box. It is important to note that this calibration procedure re-magnetizes the shield slightly, requiring that it be degaussed again by the aforementioned degaussing procedure.

d) ALTADENA[3] ^{1}H Polarization Buildup Experiment

^{1}H polarization buildup studies of VA with natural isotopic abundance (Figure 1c) were carried out by using the experimental setup described above (Figure S5). ^{1}H spectra were acquired after *para*-H_2 bubbling performed at the Earth's magnetic field and subsequent sample transfer to NMR spectrometer for detection. The representative spectrum obtained after 8 s of *para*-H_2 bubbling at the Earth's field is shown in Figure S6 (the same as inset in Figure 1c).

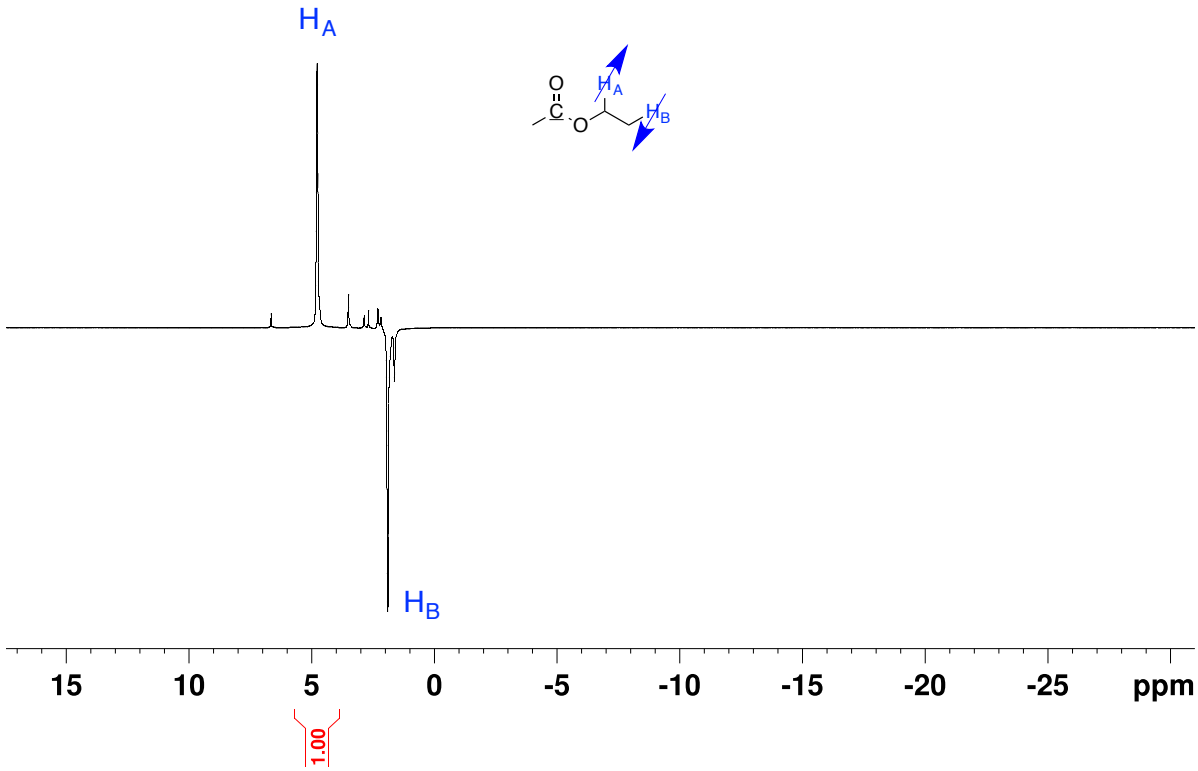

Figure S6. Typical proton NMR spectrum of ^{1}H-hyperpolarized ethyl acetate (ALTADENA condition) recorded using Bruker 400 MHz NMR spectrometer. The reaction mixture (in methanol-d_4) was obtained by bubbling *para*-H_2 (50% *para*- state, flow rate ~ 80 sccm at ~90 psi pressure, bubbling duration ~8 s) through the mixture of ~80 mM vinyl acetate and ~5 mM Rh-based catalyst (see the preparation details above).

e) Polarization Transfer From Nascent *Para*-H_2 protons to ^{13}C: B_{FC} Field Dependence

Field-cycling procedure on EA with natural ^{13}C isotopic abundance was used to find optimum field B_{FC} for polarization transfer. Figure S7 shows the representative spectrum ^{13}C with ^{1}H decoupling. It was shown that B_{FC} ~ 0.2 μT and lower provides the best polarization yield on ^{13}C carboxyl site, thus, this field was used to polarize VA-1-^{13}C substrate.

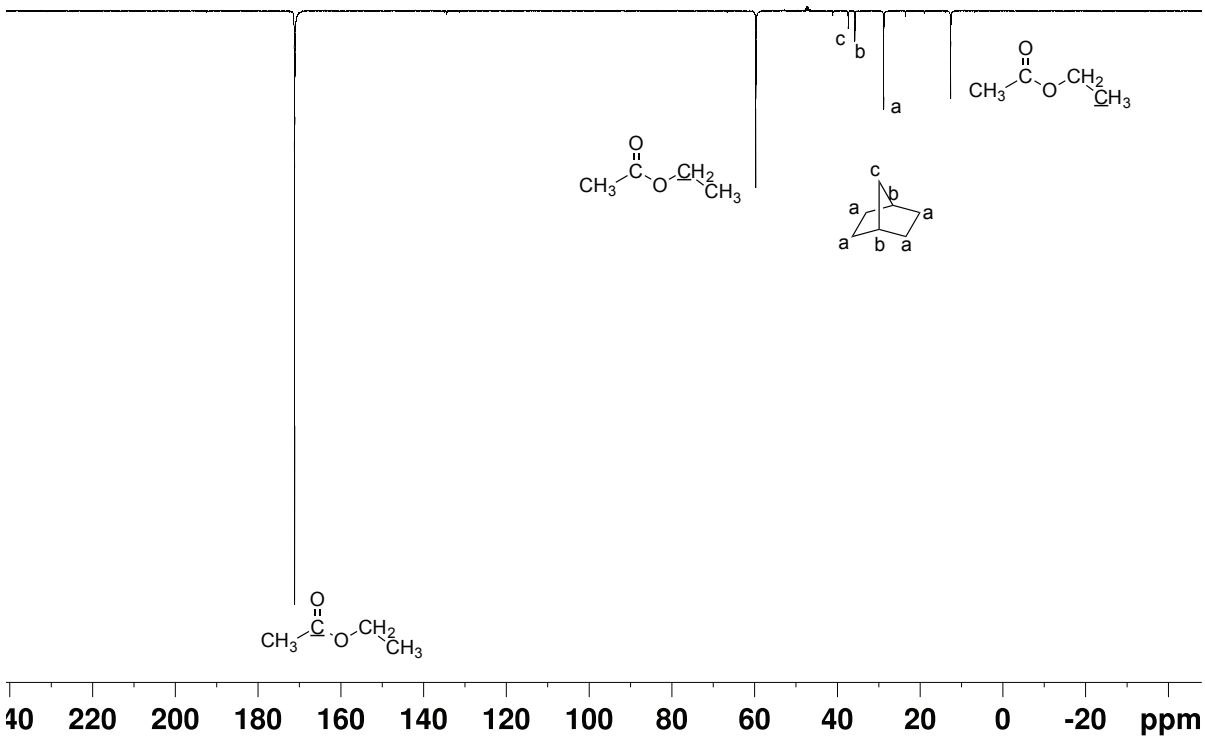

Figure S7. Typical $^{13}C\{^{1}H\}$ NMR spectrum of ^{13}C-hyperpolarized ethyl acetate (1.1% natural abundance ^{13}C of each site; note the NMR peaks of corresponding HP ^{13}C sites are labeled in HP EA and the catalyst) recorded using Bruker 400 MHz NMR spectrometer. The reaction mixture (in methanol-d_4) was obtained by bubbling *para*-H_2 (50% *para*- state, flow rate ~ 80 sccm at ~90 psi pressure, bubbling duration ~10 s) through the mixture of ~80 mM vinyl acetate and ~5 mM Rh-based catalyst (see the preparation details above), followed by the magnetic field cycling (Polarization transfer parameter, $B_{FC} \sim 0.2$ μT) and the sample transfer to 9.4 T for NMR detection.

f) ^{13}C Hyperpolarization PHIP-SAH of vinyl acetate-1-^{13}C via magnetic field cycling

VA-1-^{13}C was used to obtain hyperpolarized EA-1-^{13}C via magnetic field cycling. *Para*-H_2 bubbling was carried out in 8 s, then the sample was subjected to the field cycling procedure described above (see Figure S5).

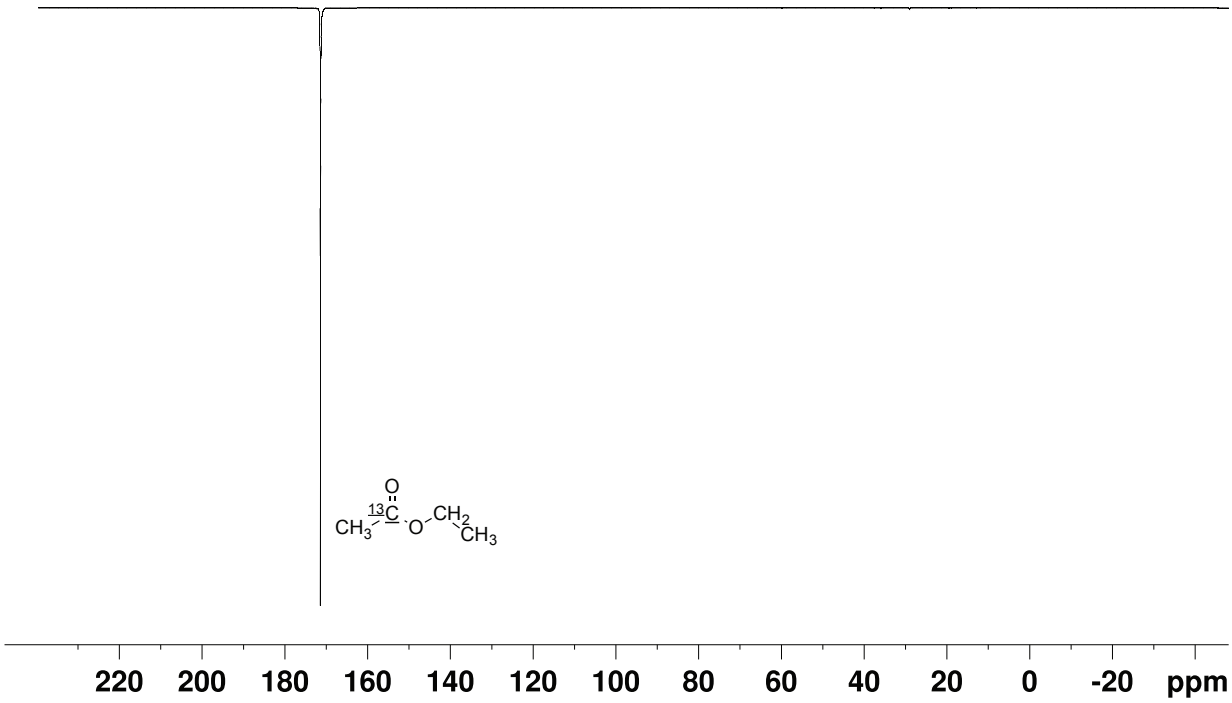

Figure S8. Typical ^{13}C{^{1}H} NMR spectrum of ^{13}C-hyperpolarized ethyl acetate-1-^{13}C recorded using Bruker 400 MHz NMR spectrometer. The reaction mixture (in methanol-d_4) was obtained by bubbling *para*-H_2 (50% *para*- state, flow rate ~ 80 sccm at ~90 psi pressure, bubbling duration ~10 s) through the mixture of ~80 mM vinyl acetate-1-^{13}C and ~5 mM Rh-based catalyst (see the preparation details above), followed by the magnetic field cycling (Polarization transfer parameter, B_{FC} ~ 0.2 μT) and the sample transfer to 9.4 T for NMR detection.

g) Calculation of Polarization Percentage for Hyperpolarized ^{1}H and ^{13}C Sites

All polarization values obtained via hydrogenation reactions were calculated with the assumption of 100% chemical conversion of vinyl acetate into ethyl acetate and vinyl acetate-1-^{13}C into ethyl acetate-1-^{13}C respectively.

Proton nuclear spin polarization, P_{1H}, of ethyl acetate (EA) produced by hydrogenation of vinyl acetate (VA) with 50% *para*-H_2 under ALTADENA conditions, was estimated by using the following equation:

$$P_{1H} = \varepsilon_{1H} \cdot P_{\text{therm}}(^{1}\text{H}) = 2 \cdot \left(\frac{S_{\text{HP}}}{S_{\text{therm}}}\right) \cdot 3.23 \cdot 10^{-5},$$

where ε_{1H} is the actual experimentally determined ^{1}H signal enhancement factor for a H_A proton (Figure 1, main text) in the -CH_2- group of EA, derived as the ratio of the hyperpolarized signal of EA (S_{HP}) and thermally polarized signal of EA after full relaxation (S_{therm}), factor of 2 takes into account that thermally polarized signal is originated from 2 protons, whereas hyperpolarized signal corresponds to one of the two *para*-H_2-nascent protons; $P_{\text{therm}}(^{1}\text{H})$ is the thermal polarization at 9.4

T at 300 K, which equals to $3.2 \cdot 10^{-5}$ or 0.0032%.

For example, P_{1H} for the sample, when the optimal bubbling time (8 s, Figure 1, main text) was used, may be calculated as the following:

$$P_{1H} = 2 \cdot \left(\frac{171.5}{0.330}\right) \cdot 3.23 \cdot 10^{-5} = 0.0332\ (3.32\%)$$
$$\text{and } \varepsilon_{1H} = 1.04 \cdot 10^{3}$$

^{13}C nuclear spin polarization P_{13C} of EA produced by pairwise *para*-H_2 addition to VA and subsequent field-cycling procedure described above, was estimated by the following equation:

$$P_{13C} = \varepsilon_{13C} \cdot P_{\text{therm}}(^{13}\text{C}) = \left(\frac{S_{\text{HP}}}{S_{\text{therm}}}\right) \cdot \left(\frac{C_{\text{therm}}}{C_{\text{HP}}}\right) \cdot 8.1 \cdot 10^{-6} \cdot 1.85$$

where ε_{13C} is the actual experimentally observed signal enhancement factor for ^{13}C site of interest, derived as the ratio of the signal of EA (S_{HP}) and the signal of thermally polarized reference sample of EA (S_{therm}), taking into account concentration difference of HP and thermally polarized sample: C_{HP} was equal to 80 mM and 80*0.011 mM for 1-^{13}C-enriched and natural abundance EA respectively, and C_{therm} was equal to 2.05 M (reference sample of sodium acetate-1-^{13}C solution); thermal polarization of ^{13}C nuclei, $P_{\text{therm}}(^{13}\text{C})$ is $8.1 \cdot 10^{-6}$ at 300 K and 9.4 T. Numerical factor of 1.85 originates from the fact that hyperpolarization by *para*-H_2 was performed in a 3.43 mm ID NMR tube (medium wall 5 mm NMR tube) with 1.6 mm OD PTFE tubing inserted inside for *para*-H_2 bubbling, while the reference spectrum for thermally polarized sample was acquired in a 4.14 mm ID standard 5 mm NMR tube causing 1.85 fold difference in effective cross section of NMR tubes in HP and thermal signal detection experiments.[4]

For example, P_{13C} for the natural abundance EA (Figure 1g) was calculated as:

$$P_{13C} = \left(\frac{12.2}{23.2}\right) \cdot \left(\frac{2.05\ \text{M}}{0.011 \cdot 0.080\ \text{M}}\right) \cdot 8.1 \cdot 10^{-6} \cdot 1.85 = 0.018\ (1.8\%)$$
$$\text{and } \varepsilon_{13C} = 2.26 \cdot 10^{3}.$$

For ^{13}C hyperpolarized EA-1-^{13}C the polarization percentage (Fig. 2h) is the following:

$$P_{13C} = \left(\frac{37.5}{0.82}\right) \cdot \left(\frac{2.05\ \text{M}}{0.98 \cdot 0.080\ \text{M}}\right) \cdot 8.1 \cdot 10^{-6} \cdot 1.85 = 0.018\ (1.8\%)$$
$$\text{and } \varepsilon_{13C} = 2.21 \cdot 10^{3}.$$

h) 3D ^{13}C MRI imaging

^{13}C 3D MRI of 80 mM HP EA-1-^{13}C (Figure 2a) and thermally polarized 4.3 M sodium acetate-1-^{13}C reference phantom (Figure 2b) were recorded using true steady state precession (true-FISP) radio-frequency (rf) pulse sequence. Both (Figure 2a and 2b) 3D true-FISP images were acquired using 15 mm OD round RF surface coil tuned to 163.5676 MHz in 15.2 T small-animal Bruker MRI scanner (Paravision 5.1) and the following acquisition parameters: spectral width (SW) = 20 kHz, TR/TE = 4.8 ms/2.4 ms, field of view (FOV) = 32×32×32 mm^3, imaging matrix = 64×64×8 resulting in voxel size of 0.5×0.5×0.5 mm^3, 10 dummy echoes, rf pulse (sinc shape) width = 1.0 ms at ~6 W corresponding to estimated 60° flip angle. Four 3D images (back-to-back) were acquired in series in ~10 s corresponding to total acquisition time ~ 2.5 s for each 3D data set. Three representative slices are shown for one of the 3D images for each sample (Figures 2a and 2b respectively).

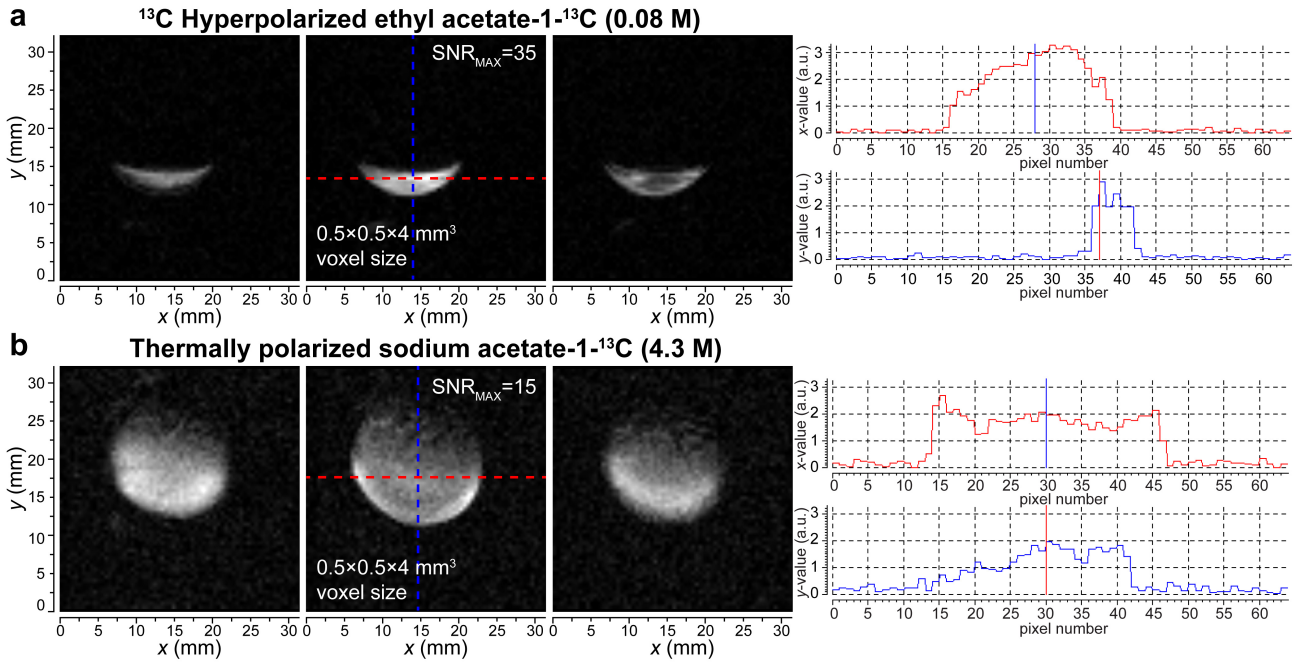

Figure S9. ^{13}C 3D MRI of (a) a hollow spherical plastic ball partially filled with 80 mM HP EA-1-^{13}C and (b) a plastic sphere (~2.8 mL) filled with thermally polarized 4.3 M sodium acetate-1-^{13}C reference phantom. Both 3D true-FISP images were acquired using 15 mm OD round RF surface coil tuned to 163.4 MHz in 15.2 T small-animal Bruker MRI scanner and the following acquisition parameters: spectral width = 20 kHz, TR/TE = 4.8 ms/2.4 ms, field of view = 32×32×32 mm^3, imaging matrix = 64×64×8, acquisition time ~ 2.5 s (see the above text for additional details). Three representative slices are shown for each 3D image.

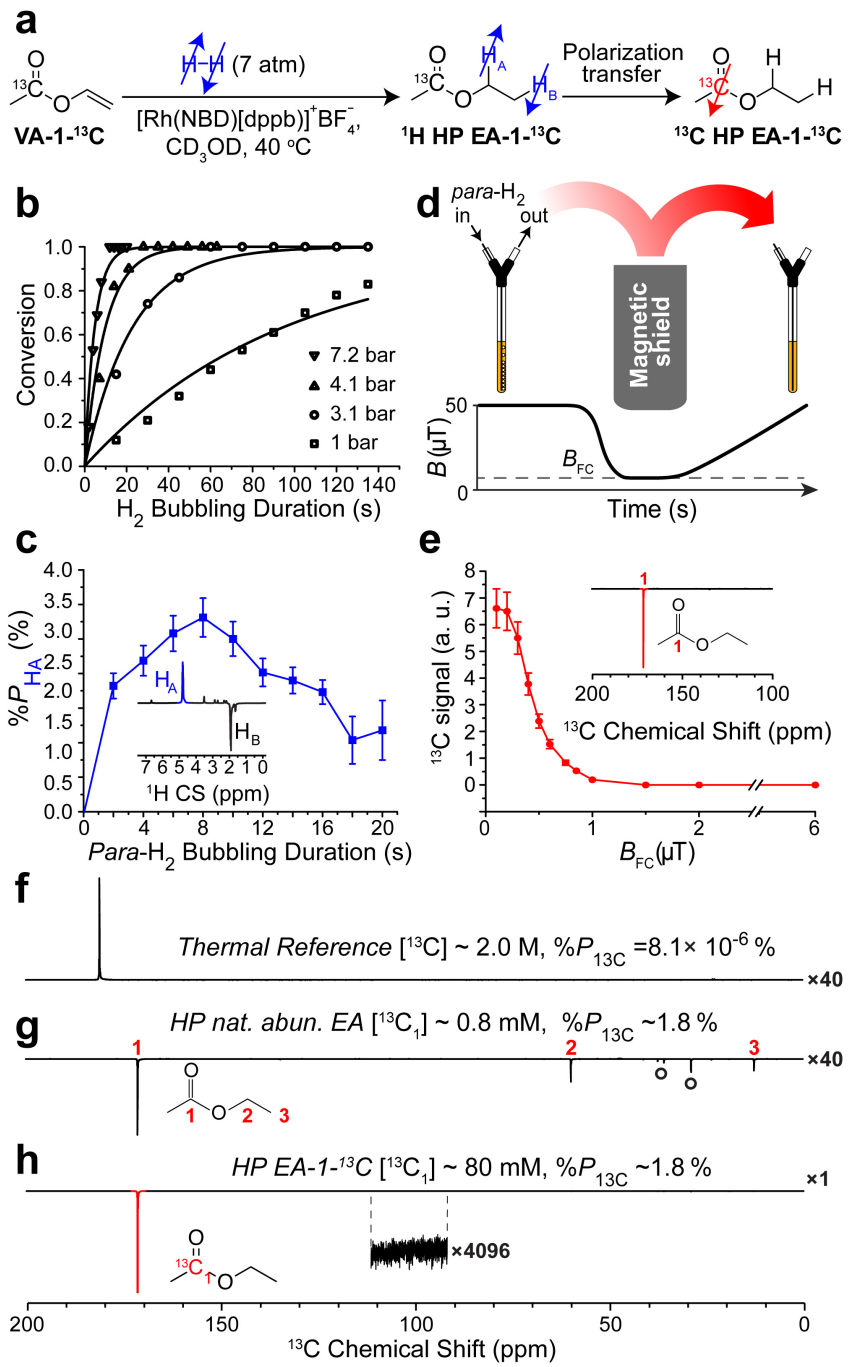

Figure S10 (color version of Figure 1, main text). a) Molecular addition of *para*-H_2 to vinyl acetate1-^{13}C (**VA-1-^{13}C**) followed by polarization transfer resulting in ^{13}C hyperpolarized ethyl acetate-1-^{13}C (**^{13}C HP EA-1-^{13}C**); **b)** Conversion profile for vinyl acetate (VA, 80 mM, in methanol-d_4, at ~40 °C temperature maintained by the 9.4 T NMR spectrometer) hydrogenation reaction in four pressure regimes; **c)** Dependence of "H_A" signal of hyperpolarized ethyl acetate (**^{1}H HP EA**) on the *para*-H_2 bubbling duration at the Earth's magnetic field (resulting in ALTADENA[24]-type spectrum shown in inset); **d)** (Top) schematic representation of experimental setup for magnetic field cycling: hydrogenation is carried out at the Earth's magnetic field, the sample then is quickly moved inside μ-metal shield (with magnetic field B_{FC}) and slowly transferred from the shield for subsequent NMR detection; (bottom) schematic magnetic field profile during the field cycling; **e)** Dependence of HP 1-^{13}C NMR signal (shown in the insert) of ethyl acetate (**^{13}C HP EA**) on the B_{FC}; **f)** Thermal spectrum of ^{13}C signal reference sodium acetate-1-^{13}C (~2.0 M).; **g)** ^{13}C HP spectrum of natural abundance 80 mM ethyl acetate (**^{13}C HP EA**). Note the resonances labeled with ° correspond to HP ^{13}C resonances originating from hydrogenation catalyst (Figure S7); **h)** HP ^{13}C spectrum of 80 mM ethyl acetate-1-^{13}C (**^{13}C HP EA-1-^{13}C**).

References Used in Supporting Information

[1] J. Ziriakus, T. K. Zimmermann, A. Pöthig, M. Drees, S. Haslinger, D. Jantke, F. E. Kühn, *Adv. Synth. Catal.* **2013**, *355*, 2845-2859.

[2] A. M. Coffey, M. L. Truong, E. Y. Chekmenev, *J. Magn. Reson.* **2013**, *237*, 169-174.

[3] M. G. Pravica, D. P. Weitekamp, *Chem. Phys. Lett.* **1988**, *145*, 255-258.

[4] D. A. Barskiy, K. V. Kovtunov, I. V. Koptyug, P. He, K. A. Groome, Q. A. Best, F. Shi, B. M. Goodson, R. V. Shchepin, M. L. Truong, A. M. Coffey, K. W. Waddell, E. Y. Chekmenev, *ChemPhysChem*, **2014**, *15*, 4100-4107.